

Unravelling the Long-lived Ligand-to-Metal Cluster Charge Transfer State in Ce-TCPP Metal Organic Frameworks

Sizhuo Yang,^a Wenhui Hu,^a James Nyakuchena,^a Christian Fiankor,^c Cunming Liu,^b Eli

Diego Kinigstein,^b Jian Zhang,^c Xiaoyi Zhang,^b Jier Huang^{a}*

^aDepartment of Chemistry, Marquette University, Milwaukee, Wisconsin, 53201

^bX-ray Science Division, Argonne National Laboratory, Argonne, Illinois, 60349

^cDepartment of Chemistry, University of Nebraska-Lincoln, Lincoln, Nebraska, 68588

Materials. (NH₄)₂Ce(NO₃)₆ (> 99.5%, Alfa Aesar), Tetrakis(4-carboxyphenyl)porphyrin (TCPP) (97%, TCI), benzoic acid (99%, Alfa Aesar), N,N-Dimethylformamide (DMF) (Certified ACS, Fisher Chemical).

The Synthesis of Ce-TCPP: Ce-TCPP was synthesized by mixing (NH₄)₂Ce(NO₃)₆ (83.2 mg, 0.15 mmol), Tetrakis(4-carboxyphenyl)porphyrin (60 mg, 0.076 mmol), and benzoic acid (490mg, 4 mmol) in DMF (6 mL) with 0.3 mL H₂O in a pressure tube. The mixture was degassed and then sonicated for 10 mins. The pressure tube was kept in oil bath at 120 °C for 48 hours. After cooling down to room temperature, the resulting solid was isolated by

centrifugation and washed with acetone 3 times. The samples were dried under vacuum before measurement. The formation of Ce-TCPP is confirmed by XRD, FT-IR and SEM.

The Synthesis of CAU-19: CAU-19 was synthesized by mixing 0.53 M aqueous $(\text{NH}_4)_2[\text{Ce}(\text{NO}_3)_6]$ solution (47 μL , 0.0253 mmol), Tetrakis(4-carboxyphenyl)porphyrin (10 mg, 0.0127 mmol) and benzoic acid (285 mg, 2.33 mmol) in DMF (6mL) with 0.15mL H_2O in a pressure tube. The pressure tube was heated at 120 $^\circ\text{C}$ for 24 h. The solid was isolated by centrifugation and washed with DMF and acetone for 3 times. The samples were dried under vacuum before measurement. The formation of CAU-19 was confirmed by XRD, FT-IR spectrum, diffuse reflectance UV-Visible spectrum, and X-ray absorption spectrum.

The Synthesis of Ce-VETTUK: Ce-VETTUK was synthesized by mixing $(\text{NH}_4)_2\text{Ce}(\text{NO}_3)_6$ (13.87 mg, 0.025 mmol), Tetrakis(4-carboxyphenyl)porphyrin (10 mg, 0.0127 mmol) and concentrated HCl (5drops) in DMF 6mL with 2.5mL H_2O in a pressure tube. The pressure tube was heated at 120 $^\circ\text{C}$ for 24 h. The solid was isolated by centrifugation and washed with DMF and acetone 3 times. The samples were dried under vacuum before measurement. The formation of VETTUK was confirmed by XRD, FT-IR spectrum, diffuse reflectance UV-Visible spectrum, and X-ray absorption spectrum.

Characterization and General Procedure. UV-Visible absorption and diffuse reflectance spectra were taken using an Agilent 8453 spectrometer equipped with Internal DRA 2500 accessories. PXRD data were collected by using Rigaku Miniflex II XRD diffractometer with Cu $\text{K}\alpha$ radiation. Scanning Electron Microscope (SEM) were taken by JSM 6510-LV (JEOL Ltd, Tokyo). Fourier-transform infrared (FT-IR) spectroscopy were measured with Nicolet iS5

FT-IR spectrometer. Gas adsorption isotherms were performed by using the surface area analyzer ASAP-2020. N₂ gas adsorption isotherms were measured at 77K using a liquid N₂ bath. Before BET measurement, samples were immersed in DMF and heated to 100°C for 24h to remove any trapped linkers, which is followed by solvent exchange with DMF, MeOH, Aceton and EtOH for 3X. Thermogravimetric Analysis (TGA) was recorded on TGA 550 Discovery series, heated from 21°C to 750°C at a rate of 8°C/minute under N₂ atmosphere. To make MOF films, the mixture of MOF with ethanol (1mg/0.5mL) was sonicated for 2 hours and then dispersed evenly on piranha-etched glass. The films were dried in air.

Femtosecond Transient Optical Absorption Spectroscopy (OTA). The OTA spectroscopy is based on a regenerative amplified Ti-Sapphire laser system (Solstice, 800nm, < 100 fs FWHM, 3.5 mJ/pulse, 1 KHz repetition rate). The tunable pump (235-1100nm), chopped at 500Hz, is generated in TOPAS from 75% of the split output from the Ti-Sapphire laser. The other 25% generated tunable UV-visible probe pulses by white light generation in a CaF₂ window (330-720 nm) on a translation stage. Helios ultrafast spectrometer (Ultrafast Systems LLC) was used to collect the spectra. The power of the pump pulse on the sample is 0.15 mW/pulse. The film samples were continuously translated to avoid heating and permanent degradation.

Steady State X-ray Absorption (XAS) spectroscopy. XAS spectra were measured at the beamline 12BM-B at the Advanced Photon Source (APS) in Argonne National Laboratory. The XAS spectra were collected under room temperature with fluorescence mode. The detector was based on 13-element germanium. One ion chamber is placed before the sample and used as the incident X-ray flux reference signal. There are two ion chambers (second and third

chambers) after the sample. The CeO₂ foil is placed between the second and third ion chambers and used for energy calibration and collecting Ce⁴⁺ spectrum. The solid samples were dispersed on Kapton tape for XAS measurement.

X-ray transient absorption (XTA) spectroscopy. XTA spectroscopy was performed at the beamline 11ID-D, APS, Argonne National Laboratory. Samples were prepared by suspending 30 mg MOFs in 70 mL acetonitrile, which is followed by sonicating for 30 mins. The 490 nm laser pump was generated by using TOPOS, which was pumped by the 800 nm from the ultrafast Ti: Sapphire laser amplifier system. The X-ray probe pulses were derived from electron bunches extracted from the storage ring. The experiment was carried out under a hybrid timing mode where an intense X-ray pulse with 16% of the total average photon flux was separated in time from other weak X-ray pulses. All X-ray bunches were used as probe pulses to extract XTA spectra at different time delays. The laser pump and X-ray probe intersect at a flowing sample stream with 550 μ m in diameter. The X-ray fluorescence signals were collected at 90° angle on both sides of the incident X-ray beam by two avalanche photodiodes (APDs). A soller slits/Ti filter combination, which was custom designed for the specific sample chamber configuration and the distance between the sample and the detector, was inserted between the sample stream and the APD detectors. The emitted Ce X-ray fluorescence collected at certain delay time (100 ps, 1 ns, 10 ns, 100 ns) after the laser pump pulse excitation was used to build the laser-on spectrum in APS hybrid mode. 70 scans of the difference spectrum were averaged for 100ps, 1ns, 10ns delay, 25 scans for 100ns delay due to time limitation.

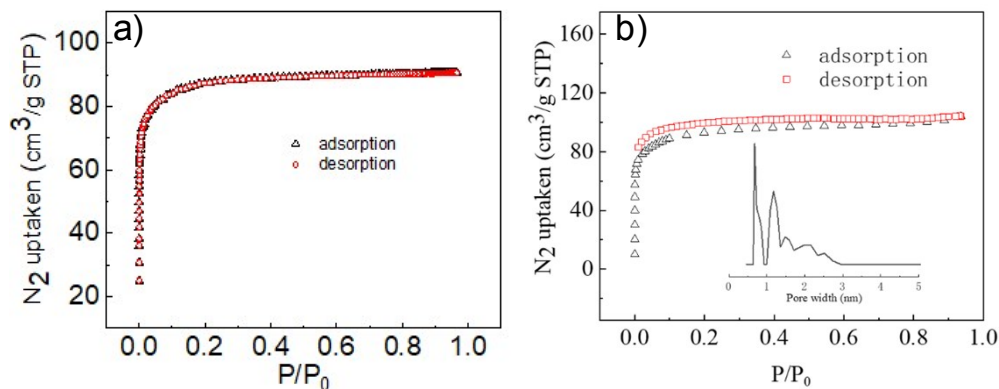


Figure S1. N₂ adsorption/desorption isotherm of Ce-TCPP based on two measurements, where the surface area is determined to be 332.56 (a) and 352.77m²/g (b). The inset of (b) shows the pore size distribution, which indicates the average pore width of 1.82 nm.

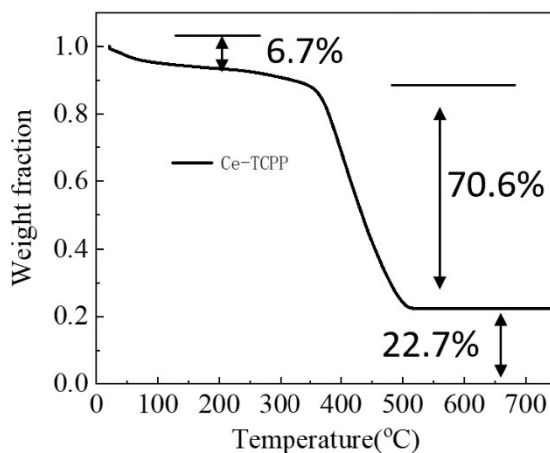


Figure S2. TGA of Ce-TCPP after CO₂ activation. In this experiment, all lattice incorporated solvents in Ce-TCPP have been removed after CO₂ activation which was performed before TGA measurement. The weight loss below 100°C is assigned to the evaporation of water molecules. The weight loss around 400°C is attributed to the break down of the Ce-O bond.

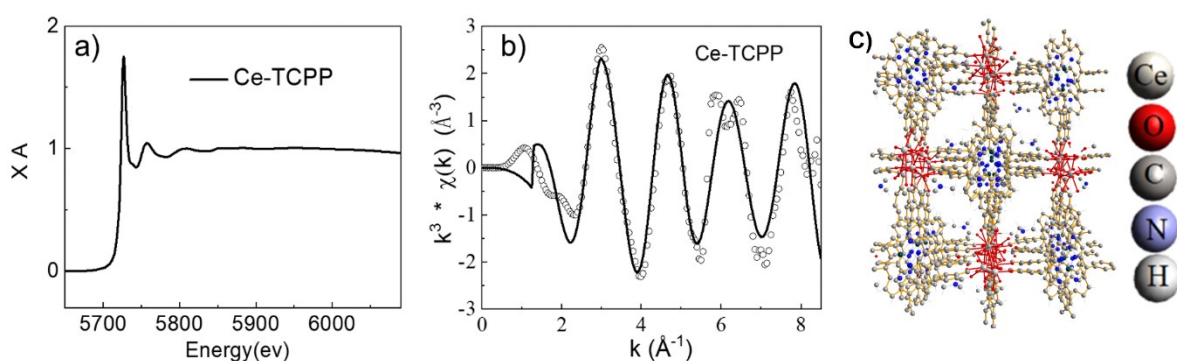


Figure S3. Full EXAFS spectra (a) and the Fourier-transformed k-space (b) spectra of Ce-TCPP. The data are shown as open points and FEFF fits as solid lines. (c) The fitting model of Ce-TCPP.

Table S1. EXAFS fitting results for Ce-TCPP, CAU-19 and VETTUK. The structural parameters were obtained by the least-squares curve parameter method via Artemis. The corresponding fit figure is shown in Figure S3. The six entries (Co-O single scattering path) were included due to high rank in the FEFF calculation. Fitting model is generated based on a reported structure (CCDC 612945) and is visualized in Figure 2b and Figure S3c. The fitting was done in both R space and K space with application of k^3 weights. The EXAFS data were Fourier transformed over the ranges $2.544 < K < 8.149 \text{ \AA}^{-1}$ (Ce-TCPP), $2.599 < K < 8.120 \text{ \AA}^{-1}$ (CAU-19), $2.543 < K < 8.148 \text{ \AA}^{-1}$ (VETTUK) and $1 < R < 2.8 \text{ \AA}$ for all fits. Additional parameters: Ce-TCPP $\Delta E_0 = 6.28$, CAU-19 $\Delta E_0 = 3.64$, VETTUK $\Delta E_0 = 2.30$, S_0^2 was fixed to 1 (all paths).

Ce-TCPP			
vector	N	R(Å)	$\sigma^2 \times 10^{-3} (\text{\AA}^2)$
Ce-O ₁	1	2.22(+/- 0.02)	7.7
Ce-O ₂	3	2.44(+/- 0.02)	1
Ce-O ₃	4	2.61(+/- 0.02)	9.9

CAU-19			
vector	N	R(Å)	$\sigma^2 \times 10^{-3} (\text{\AA}^2)$
Ce-O ₁	2	2.23(+/- 0.02)	6.8
Ce-O ₂	8	2.48(+/- 0.02)	5.2
Ce-O ₃	6	2.72(+/- 0.02)	10

VETTUK			
vector	N	R(Å)	$\sigma^2 \times 10^{-3} (\text{\AA}^2)$
Ce-O ₁	1	2.25(+/- 0.02)	10
Ce-O ₂	3	2.42(+/- 0.02)	1
Ce-O ₃	4	2.56(+/- 0.02)	3.2

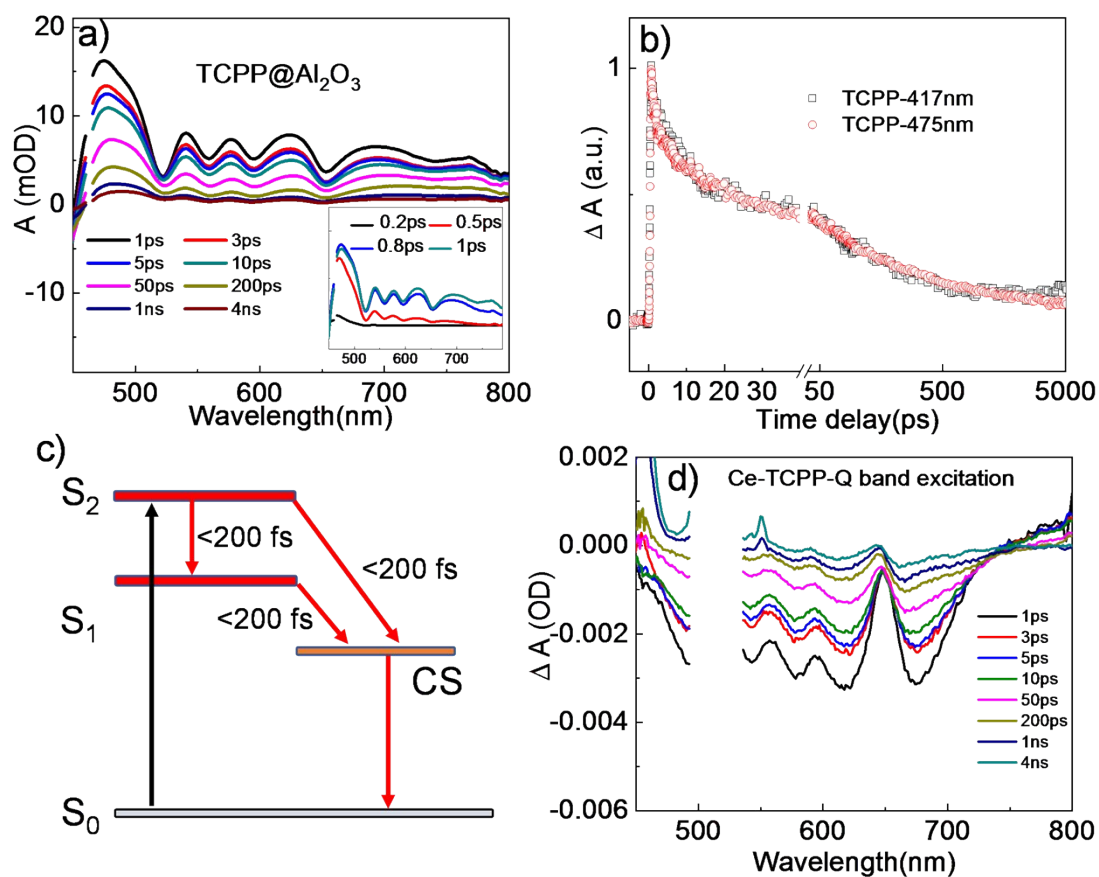


Figure S4. (a) Femtosecond OTA spectra of TCPP on Al_2O_3 film. (b) Comparison of ES decay and ground-state bleach recovery of TCPP on Al_2O_3 film. GSB recovery at 417 nm was reversed for better comparison. (c) Energetic diagram of Ce-TCPP following 400 nm excitation. (d) Femtosecond OTA spectra of Ce-TCPP with Q band excitation

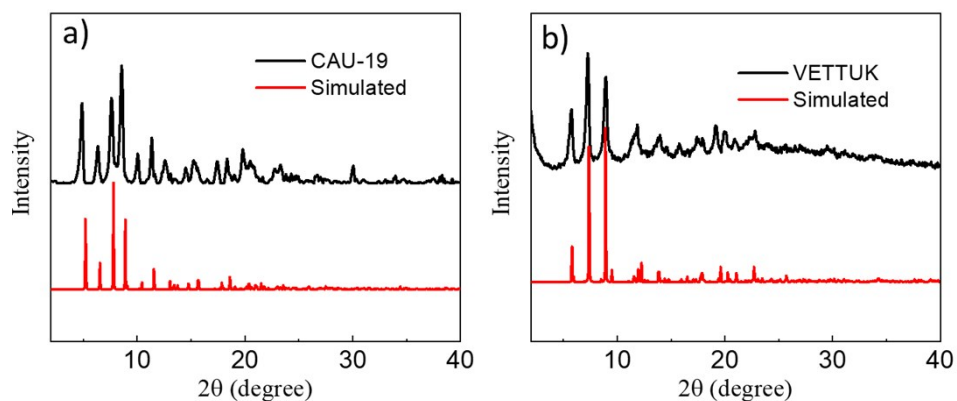


Figure S5. XRD patterns of (a) CAU-19 and (b) Ce-VETTUK

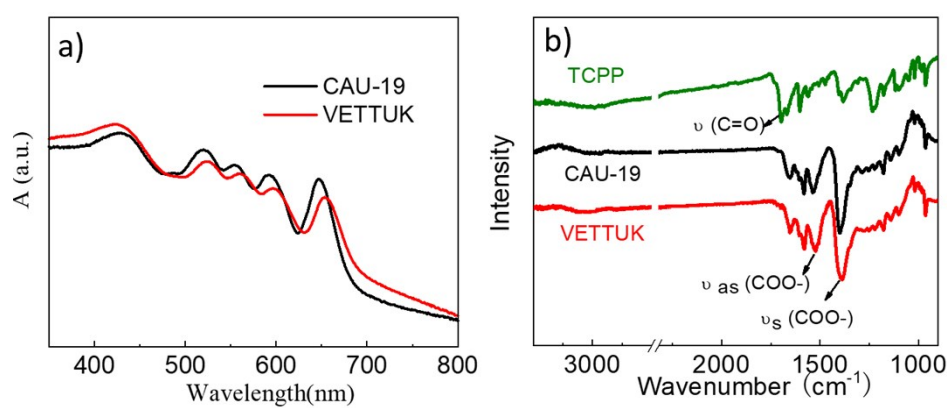


Figure S6. (a) The diffuse reflectance spectrum of CAU-19 (black) and Ce-VETTUK (red). (b) FT-IR spectra of CAU-19 (black), Ce-VETTUK (red) and TCPP (olive).

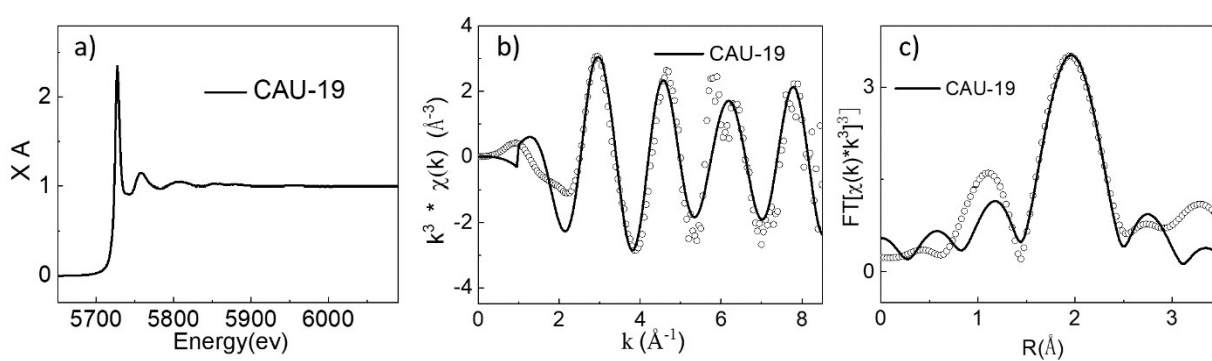


Figure S7. Full EXAFS spectra (a), the Fourier-transformed k-space (b) spectra and the Fourier-transformed R-space (c) spectra of CAU-19.

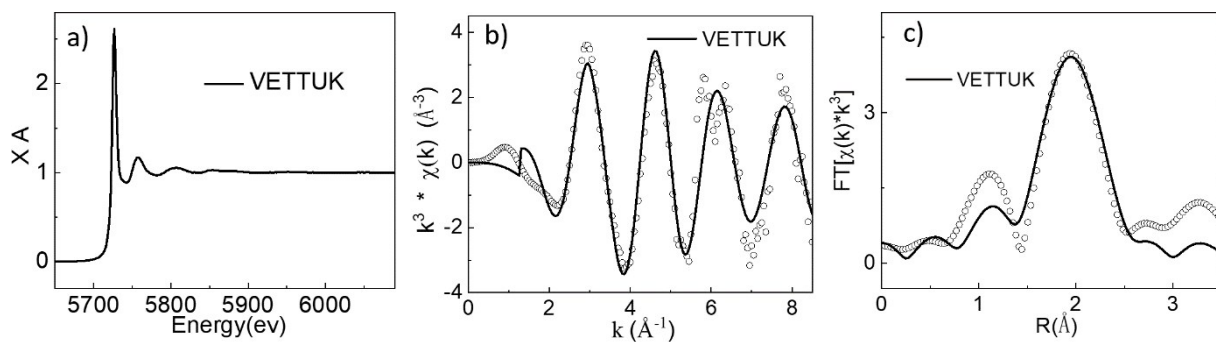


Figure S8. Full EXAFS spectra (a), the Fourier-transformed k -space (b) spectra and the Fourier-transformed R -space (c) spectra of Ce-VETTUK.

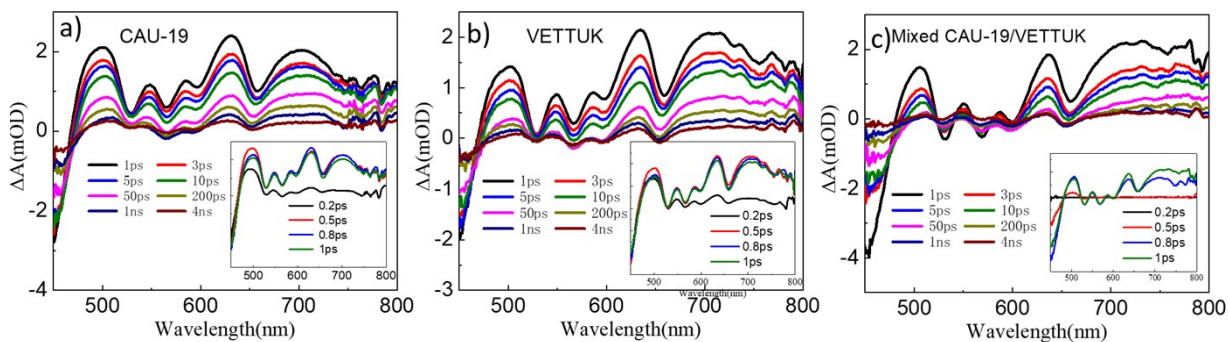


Figure S9. Femtosecond OTA spectra of (a) CAU-19, (b) Ce-VETTUK and (c) Mixed CAU-19 and Ce-VETTUK in 1:1 ratio.

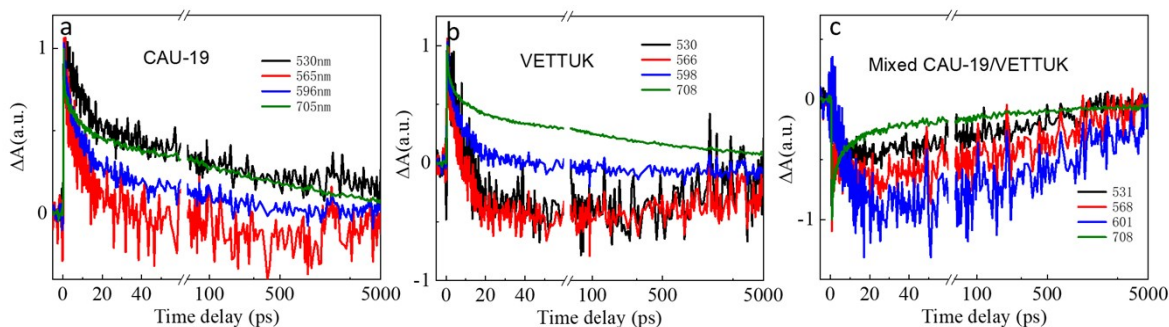


Figure S10. The kinetic traces of Q band ground state bleach (GSB) recovery of (a) CAU-19, (b) Ce-VETTUK and (c) Mixed CAU-19 and Ce-VETTUK in 1:1 ratio

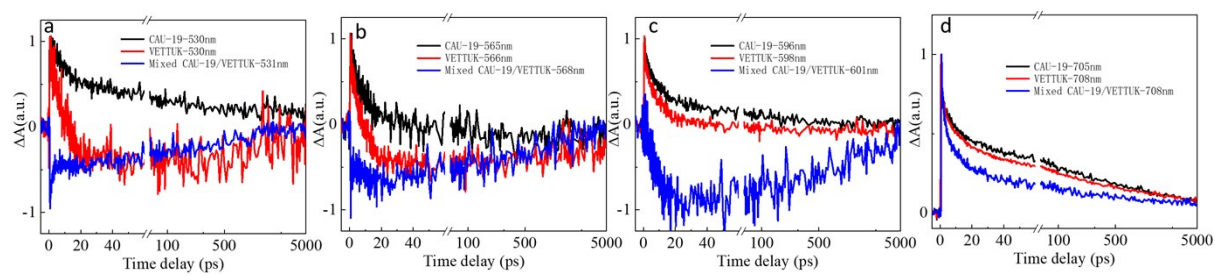


Figure S11. The comparison of kinetic traces of CAU-19, VETTUK and Mixed CAU-19/VETTUK at different probe wavelengths